

# Note of Caution for the Aqueous Behaviour of Metal-based Drug Candidates

*Anna Notaro,<sup>a</sup> Gilles Gasser,<sup>a,\*</sup> and Annie Castonguay<sup>b,\*</sup>*

<sup>a</sup> Chimie ParisTech, PSL University, CNRS, Institute of Chemistry for Life and Health Sciences, Laboratory for Inorganic Chemical Biology, F-75005 Paris, France.

<sup>b</sup> INRS - Centre Armand-Frappier Santé Biotechnologie, Organometallic Chemistry Laboratory for the Design of Catalysts and Therapeutics, Université du Québec, 531 boul. des Prairies, Laval, Québec, H7V 1B7, Canada.

\* Corresponding authors: E-mail: [gilles.gasser@chimeparistech.psl.eu](mailto:gilles.gasser@chimeparistech.psl.eu); WWW: [www.gassergroup.com](http://www.gassergroup.com); Phone: +33 1 44 27 56 02; Email: [annie.castonguay@inrs.ca](mailto:annie.castonguay@inrs.ca); WWW: [www.castonguay-group-inrs.com/](http://www.castonguay-group-inrs.com/) Phone: +1 450 687 5010

ORCID Number

Anna Notaro: 0000-0003-0148-1160

Gilles Gasser: 0000-0002-4244-5097

Annie Castonguay: 0000-0001-5705-6353

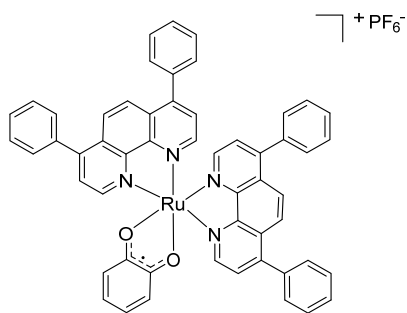
**Keywords:** Aqueous Behaviour, Bioinorganic Chemistry, Cancer, Medicinal Inorganic Chemistry, Ruthenium.

## Abstract

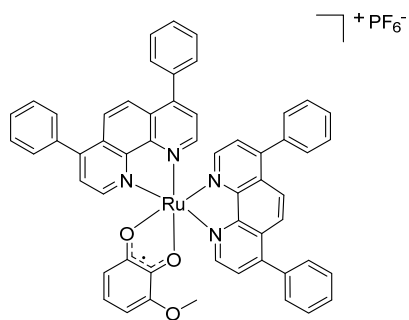
Poor aqueous solubility is one of the recurrent drawbacks of many compounds in medicinal chemistry. To overcome this limitation, the dilution of drug candidates from stock solutions is common practice. However, the precise characterisation of these compounds in aqueous solutions is often neglected, leading to some uncertainties regarding the nature of the actual active species. In this communication, we demonstrate that two ruthenium complexes previously reported by our group for their chemotherapeutic potential against cancer, namely  $[\text{Ru}(\text{DIP})_2(\text{sq})](\text{PF}_6)$  and  $[\text{Ru}(\text{DIP})_2(3\text{-methoxysq})](\text{PF}_6)$ , where DIP is 4,7-diphenyl-1,10-phenanthroline, sq = semiquinonate and 3-methoxysq = 3-methoxysemiquinonate, form colloids in water-DMSO (1% v/v) mixtures that are invisible to the naked eyes.  $[\text{Ru}(\text{DIP})_2(3\text{-methoxysq})](\text{PF}_6)$  was found to form a highly stable and monodispersed colloid with nanoaggregates of  $\sim 25$  nm. In contrast,  $[\text{Ru}(\text{DIP})_2(\text{sq})](\text{PF}_6)$  was found to form large reticulates of mostly spherical aggregates which size was found to increase over time. The difference in size and shape distribution of drug candidates is of tremendous significance as the study of their biological activity might be severely affected. Overall, we strongly believe that these observations should be taken into account by the scientific community working on the development of metal-based drugs with poor water solubility.

## Introduction

The choice of an appropriate solvent to accomplish a specific task is often guided by the rule of thumbs as “like dissolves like”.<sup>[1]</sup> Many parameters have been defined over the years to describe the concept of solubility, but it is commonly accepted that a solution is an homogeneous mixture of two or more substances, which include a solvent (i.e. the component present in the largest amount) and a solute (i.e. the component present in the smallest amount).<sup>[1]</sup> Any further detailed explanation about this topic is beyond the scope of this communication.<sup>[1]–[4]</sup> When the solute is not dissolved by the solvent, an heterogeneous mixture is formed, which can either be identified as a suspension or a colloid.<sup>[5],[6]</sup> A suspension is characterised by particles usually larger than 1  $\mu\text{m}$ , that might be visible to the naked eye and suitable for sedimentation,<sup>[6]</sup> whereas a colloid corresponds to a dispersed phase of smaller particles (1-1000 nm) that do not settle.<sup>[5]</sup> Herein, we describe the water-DMSO mixture (1% v/v) behaviour of two ruthenium polypyridyl complexes previously reported by our group as potential chemotherapeutic agents against cancer, namely **[Ru(DIP)<sub>2</sub>(sq)](PF<sub>6</sub>)** and **[Ru(DIP)<sub>2</sub>(3-methoxysq)](PF<sub>6</sub>)**, where DIP is 4,7-diphenyl-1,10-phenanthroline, sq = semiquinonate and 3-methoxysq = 3-methoxysemiquinonate (Figure 1).<sup>[7],[8]</sup> The formation of ruthenium polypyridyl nanoaggregates is a known phenomenon.<sup>[9]–[16]</sup> For example, the formation of nanoaggregates of **[Ru(DIP)<sub>3</sub>]<sup>2+</sup>** and **[Ru(bpy)<sub>3</sub>]<sup>2+</sup>** in water was previously reported in the literature. However, overall, data currently available in the literature on this topic is relatively scarce.<sup>[9],[10]</sup> In this communication, we demonstrate that **[Ru(DIP)<sub>2</sub>(sq)](PF<sub>6</sub>)** and **[Ru(DIP)<sub>2</sub>(3-methoxysq)](PF<sub>6</sub>)** form colloids in a water-DMSO mixture (1% v/v) and that their slight structural difference has a dramatic effect on their self-assembly, a process by which pre-existing components autonomously organise into patterns or structures.<sup>[17],[18]</sup>



**[Ru(DIP)<sub>2</sub>(sq)](PF<sub>6</sub>)**



**[Ru(DIP)<sub>2</sub>(3-methoxysq)](PF<sub>6</sub>)**

**Figure 1.** Chemical structures of **[Ru(DIP)<sub>2</sub>(sq)](PF<sub>6</sub>)** and **[Ru(DIP)<sub>2</sub>(3-methoxysq)](PF<sub>6</sub>)** previously published by our group.<sup>[7],[8]</sup>

## Results and discussion

**[Ru(DIP)<sub>2</sub>(sq)](PF<sub>6</sub>)** and **[Ru(DIP)<sub>2</sub>(3-methoxysq)](PF<sub>6</sub>)** have been recently reported by our group for their remarkable potential as chemotherapeutic agents against cancer.<sup>[7],[8]</sup> During follow-up experiments, we observed an interesting behaviour of these compounds upon aqueous dilution from DMSO stock solutions. As already reported by our group and others, although widely used, DMSO can be found problematic for the biological assessment of metal complexes due to its coordinative properties.<sup>[19]-[21]</sup> However, in this case, the stability of **[Ru(DIP)<sub>2</sub>(sq)](PF<sub>6</sub>)** and **[Ru(DIP)<sub>2</sub>(3-methoxysq)](PF<sub>6</sub>)** in DMSO was found to be very high, the nature of both compounds remaining unaltered up to at least 4 days.<sup>[7],[8]</sup> In this communication, we describe the behaviour of **[Ru(DIP)<sub>2</sub>(sq)](PF<sub>6</sub>)** and **[Ru(DIP)<sub>2</sub>(3-methoxysq)](PF<sub>6</sub>)** in water-DMSO (1% v/v) mixtures that we believe will be of interest for the scientists working in the medicinal inorganic chemistry field of research. More specifically, **[Ru(DIP)<sub>2</sub>(sq)](PF<sub>6</sub>)** and **[Ru(DIP)<sub>2</sub>(3-methoxysq)](PF<sub>6</sub>)** were found to form colloids that are completely transparent and consequently, unnoticeable to the naked eye. Many techniques are known nowadays to characterise clusters or aggregates of ruthenium complexes (e.g., NMR or mass spectrometry techniques).<sup>[22]-[24]</sup> However, conventional methods for solubility screens (e.g., UV-vis absorbance) could have easily led to the misidentification of these colloids as solutions, especially if a non-instinctive fine filtration step would have been skipped. The first attempt to assess the solubility of **[Ru(DIP)<sub>2</sub>(sq)](PF<sub>6</sub>)** and **[Ru(DIP)<sub>2</sub>(3-methoxysq)](PF<sub>6</sub>)** in water-DMSO (1% v/v) was performed by comparing the UV absorbance of each compound with a calibration curve (response vs concentration) prepared in the same media.<sup>[25]</sup> It is expected that a calibration curve should be linear when the compound is completely soluble at the lowest concentrations tested, and reach a plateau for saturated solutions

of higher concentrations, for which precipitation occurs.<sup>[25]</sup> Normally, solutions are filtered to prevent any interference of the precipitate with the analysis. In the case of the two above-mentioned compounds, a linear calibration curve was observed for the non-filtered solutions (5, 2.5, 1 and 0.5  $\mu\text{M}$ , Figure S1, S2). At all concentrations tested, no precipitate was noticeable to the naked eye, whereas inconsistent results were obtained when solutions were filtered using 0.2  $\mu\text{m}$  cellulose acetate membrane filters (VWR) prior to analysis. These findings brought us to doubt the composition of what we identified so far as a ‘solution’. The next step towards the understanding of the behaviour of **[Ru(DIP)<sub>2</sub>(sq)](PF<sub>6</sub>)** and **[Ru(DIP)<sub>2</sub>(3-methoxysq)](PF<sub>6</sub>)** in water-DMSO (1% v/v) was undertaken using nanoparticle tracking analysis (NTA) performed with a Nanosight NS300 instrument (Malvern Panalytical).<sup>[26],[27]</sup> NTA is a nanoparticle visualisation technique that allows size, count and concentration measurements.<sup>2</sup> One of the major advantages of this technique, compared to classical dynamic light scattering (DLS), is that it can successfully resolve and accurately measure different particle sizes in its range of acquisition (10 nm to 2000 nm).<sup>[27]</sup> DLS measures changes in light scattering from a bulk sample whereas NTA provides particle-by-particle diffusion measurements and builds the distribution one particle at a time.<sup>2</sup> However, samples must be concentrated enough ( $10^6$ - $10^9$  particles per mL) to provide measurements of statistical relevance.<sup>[28]</sup> NTA measurements of **[Ru(DIP)<sub>2</sub>(sq)](PF<sub>6</sub>)** and **[Ru(DIP)<sub>2</sub>(3-methoxysq)](PF<sub>6</sub>)** (1  $\mu\text{M}$ ) in a water-DMSO (1% v/v) mixture were attempted. Samples were prepared by diluting DMSO stock solutions (100  $\mu\text{L}$  of 100  $\mu\text{M}$  solutions) with milliQ water (9.90 mL) immediately prior to analysis. Samples were analysed at  $t = 0$  and after 24 h incubation at 28 °C. Analysis of complex **[Ru(DIP)<sub>2</sub>(sq)](PF<sub>6</sub>)** was considered unreliable by NTA as not enough particles were detected. This could be explained by the presence of large aggregates or by the partial

solubility of the complex in this media. On the other hand,  $[\text{Ru}(\text{DIP})_2(3\text{-methoxysq})](\text{PF}_6)$  was accurately analysed by NTA showing a surprisingly monodispersed distribution with aggregates of  $\sim 42$  nm (Figure S3). Those aggregates were not found to be stable after being incubated at  $28^\circ\text{C}$  for 24 h, as two main population distributions of  $\sim 65$  nm and  $\sim 95$  nm were observed (Figure S4). It is noteworthy that despite their extremely similar structure, as reflected by their very close physical properties,<sup>[7],[8]</sup> the NTA analysis of  $[\text{Ru}(\text{DIP})_2(\text{sq})](\text{PF}_6)$  and  $[\text{Ru}(\text{DIP})_2(3\text{-methoxysq})](\text{PF}_6)$  gave significantly different results. This interesting finding prompted us to investigate these systems more deeply using transmission electron microscopy (TEM). Figure 2 shows TEM images of  $[\text{Ru}(\text{DIP})_2(\text{sq})](\text{PF}_6)$  and  $[\text{Ru}(\text{DIP})_2(3\text{-methoxysq})](\text{PF}_6)$  at  $t = 0$  and after 24 h incubation at  $28^\circ\text{C}$ .

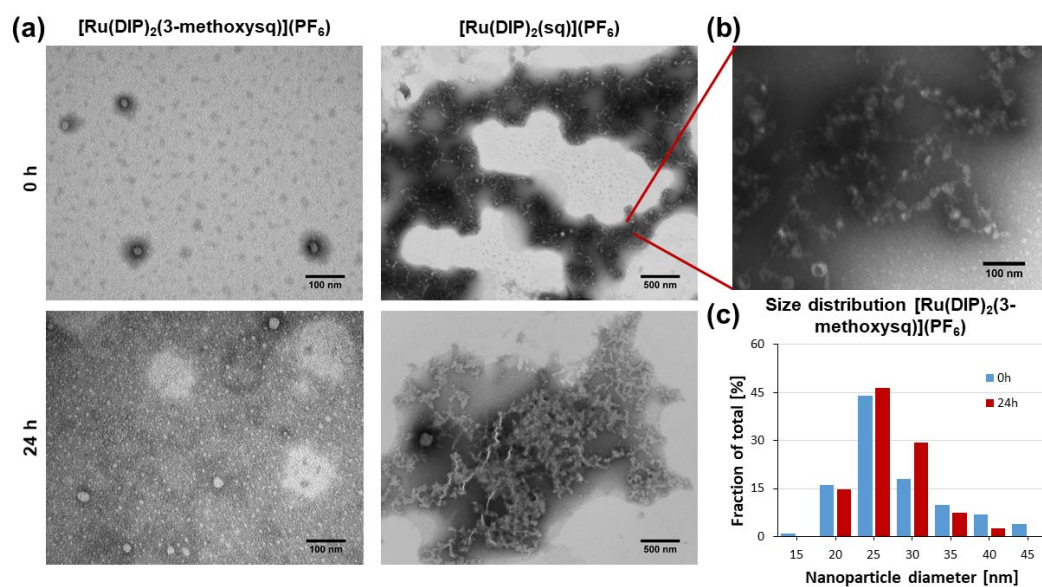


**Figure 2.** (a) TEM images of  $[\text{Ru}(\text{DIP})_2(3\text{-methoxysq})](\text{PF}_6)$  and  $[\text{Ru}(\text{DIP})_2(\text{sq})](\text{PF}_6)$  at  $t = 0$  and after 24 h incubation at  $28^\circ\text{C}$ . (b) Zoom-in of the  $[\text{Ru}(\text{DIP})_2(\text{sq})](\text{PF}_6)$  image at  $t = 0$ . (c) Size distribution of  $[\text{Ru}(\text{DIP})_2(3\text{-methoxysq})](\text{PF}_6)$  at  $t = 0$  and after 24 h incubation at  $28^\circ\text{C}$ .

TEM analysis of  $[\text{Ru}(\text{DIP})_2(\text{sq})](\text{PF}_6)$  revealed immediate formation of fine reticulates of mostly spherical nanoaggregates, which increased in size over time ( $>1 \mu\text{m}$ ). The size of the nanoaggregates was difficult to establish, especially after 24 h, when the level of aggregation was more considerable. However, image *J* analysis of the image at  $t = 0$  demonstrates that the size of the nanoaggregates did not exceed 50 nm. On the other hand, the TEM analysis of  $[\text{Ru}(\text{DIP})_2(3\text{-methoxysq})](\text{PF}_6)$  showed isolated spherical nanoaggregates. A remarkably low size polydispersity at  $t = 0$  ( $25.3 \pm 6.3 \text{ nm}$ ) and at  $t = 24 \text{ h}$  ( $24.6 \pm 4.3 \text{ nm}$ ) was also observed, showing a stability of the system over time, under the conditions tested. Table 1 summarises the data obtained for  $[\text{Ru}(\text{DIP})_2(\text{sq})](\text{PF}_6)$  and  $[\text{Ru}(\text{DIP})_2(3\text{-methoxysq})](\text{PF}_6)$  by NTA and TEM. As expected, NTA showed particles of a relatively larger size as this analysis includes a measurement of the aggregates' hydrodynamic radius.

**Table 1.** NTA and TEM data obtained for  $[\text{Ru}(\text{DIP})_2(\text{sq})](\text{PF}_6)$  and  $[\text{Ru}(\text{DIP})_2(3\text{-methoxysq})](\text{PF}_6)$  at  $t = 0$  and after 24 h incubation at  $28 \text{ }^\circ\text{C}$ .

	NTA most frequent size(s)		TEM mean size $\pm$ s.d.	
	t = 0	t = 24 h	t = 0	t = 24 h
$[\text{Ru}(\text{DIP})_2(\text{sq})](\text{PF}_6)$	n.a.	n.a.	$>1 \mu\text{m}$	$>1 \mu\text{m}$
$[\text{Ru}(\text{DIP})_2(3\text{-methoxysq})](\text{PF}_6)$	41.9 nm	65 nm, 95 nm	$25.3 \pm 6.3 \text{ nm}$	$24.6 \pm 4.3 \text{ nm}$

These results demonstrate that compounds that appear completely soluble to the naked eye and display a linear relationship when their UV absorbance is measured versus their concentration might actually be in the form of colloids. Moreover, this study shows that

minor changes in the chemical structure of some compounds might lead to a dramatic change in their self-assembly.

## **Conclusion**

Overall, this study demonstrates how “clear solutions” that result in linear UV absorption calibration curves can actually be dispersions of colloidal nature. One of the most widely used techniques to assess the solubility of a compound is to verify the linearity of its UV absorbance in solution versus concentration, as expressed by the Beer-Lambert law. In the course of this study, we demonstrated that two structurally-related Ru(II)polypyridyl complexes form nanoparticles or nanoaggregates in water-DMSO media that were completely unnoticeable to the naked eye. Therefore, their solubility assessment by a conventional technique such as UV could have easily led to a misassumption, if solutions remained unfiltered prior to analysis. In the case of both compounds investigated in this study, inconsistent results were obtained after filtrating the solutions. These findings emphasise the crucial importance of this “sometimes not instinctive” filtration step for solubility assessment, as well as the use supplementary characterisation tools. A deeper investigation using NTA and TEM analyses was undertaken and showed that the small difference between the structure of both complexes caused dramatic effect on their self-assembly, going from well-defined reticulate to isolated nanoaggregates. We believe these findings might prompt the medicinal inorganic chemistry community to invest more efforts towards the characterisation of metallic compounds prior to their biological activity assessment. Indeed, a full characterisation of metal-based drug candidates of interest under relevant conditions would contribute to prevent any uncertainty regarding the actual biologically active species. For example, the observations reported herein could rationalize

differences in *in vivo* results between two very similar compounds due to the enhanced permeability and retention effect (EPR effect), although this concept is currently controversial.<sup>[29],[30]</sup>

## **Experimental Section**

### **Materials**

All chemicals (reagent or analytical grade) were used as received from commercial sources.  $[\text{Ru}(\text{DIP})_2(\text{sq})](\text{PF}_6)$  and  $[\text{Ru}(\text{DIP})_2(3\text{-methoxysq})](\text{PF}_6)$  were synthesised in our laboratories.<sup>[7],[8]</sup> All solvents were purchased (analytical or HPLC grade) and when necessary, degassed by purging with dry, oxygen-free nitrogen for at least 30 min before use.

### **Instrumentation and methods**

#### **UV Absorption**

Samples were prepared starting from 1 mM stock solutions of  $[\text{Ru}(\text{DIP})_2(\text{sq})](\text{PF}_6)$  and  $[\text{Ru}(\text{DIP})_2(3\text{-methoxysq})](\text{PF}_6)$  in DMSO. Further dilutions were made in order to allow the preparation of 10 mL aqueous solutions containing 1% DMSO in volume at 5  $\mu\text{M}$ , 2.5  $\mu\text{M}$ , 1  $\mu\text{M}$  and 0.5  $\mu\text{M}$ . The solutions were then measured in a 96-well plate (200  $\mu\text{L}$ ), using a SpectraMax M5 microplate reader. Data were analysed by Microsoft excel.

#### **Nanoparticle tracking analysis (NTA)**

NTA was performed using Nanosight NS300 (Malvern). Samples were prepared starting from 1 mM stock solutions of  $[\text{Ru}(\text{DIP})_2(\text{sq})](\text{PF}_6)$  and  $[\text{Ru}(\text{DIP})_2(3\text{-methoxysq})](\text{PF}_6)$  in DMSO. A 1 mM stock solution was further diluted to 0.1 mM in DMSO and 0.1 mL was diluted with 9.9 mL of milliQ water immediately prior to analysis. Each solution was injected automatically with the Nanosight syringe pump

add-on (0.2 mL) at a rate of 50  $\mu$ L/s. Compounds were then incubated at 28 °C in a 6-well plate and the analysis repeated after 24 h.

### **Transmission electron microscopy (TEM)**

Solutions were prepared as explained above, then a 50  $\mu$ L drop of the sample was placed on parafilm. Grids (200mesh copper with FORMVAR plastic (as a support film), carbon coated and glow discharged) were then placed on the drop for 5 min and dried with a bibulous paper. Samples were treated with Phosphotungstic acid (PTA) 3% for 1 min, then dried with bibulous paper. Finally, grids loaded with the samples were analysed using TEM Hitachi H-7100 at 75K with a camera AMT X111 (Service de microscopie électronique, INRS).

### **Associated Content**

#### **Supporting Information**

The Supporting Information is at DOI: XXXXX.

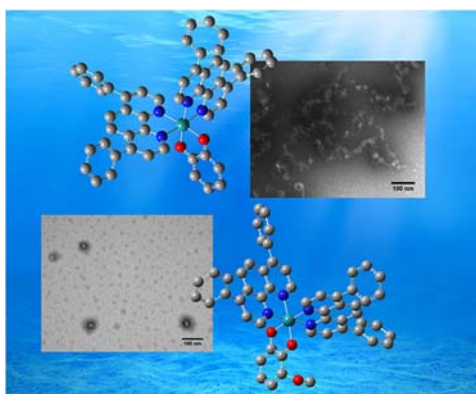
Calibration curve of **[Ru(DIP)<sub>2</sub>(sq)](PF<sub>6</sub>)** (Figure S1), calibration curve of **Ru(DIP)<sub>2</sub>(3-methoxysq)](PF<sub>6</sub>)** (Figure S2), NTA size distribution at t = 0 of and **[Ru(DIP)<sub>2</sub>(3-methoxysq)](PF<sub>6</sub>)** (Figure S3), NTA size distribution after 24 h incubation at 28 °C of and **[Ru(DIP)<sub>2</sub>(3-methoxysq)](PF<sub>6</sub>)** (Figure S4).

### **Acknowledgements**

This work was financially supported by an ERC Consolidator Grant PhotoMedMet to G.G. (GA 681679) and has received support under the program *Investissements d'Avenir* launched by the French Government and implemented by the ANR with the reference ANR-10-IDEX-0001-02 PSL (G.G.). Ile de France Region is gratefully acknowledged for financial support of 500 MHz NMR spectrometer of Chimie

ParisTech in the framework of the SESAME equipment project. We acknowledge the loan of Agilent's equipment to Chimie ParisTech. This work was also supported by INRS University, the Natural Sciences and Engineering Research Council of Canada (Discovery 06336 to A.C.), the Fonds de Recherche du Québec Santé (Junior 1 Research Scholar, Établissement de Jeunes Chercheurs 32622 to A.C.) and the Canada Foundation for Innovation (John Evans Leaders Fund 34846 to A.C.). We would like to thank Prof. Charles Ramassamy and his team (INRS) for providing access and technical assistance for the use of the Nanosight NS300 instrument as well as the Louise Frappier Foundation for the acquisition of this equipment.

## TOC



## References

- [1] Burke, J. B. *Pap. Gr. Annu.* **1984**, *3*, 1–30.
- [2] Hansen, C. M. *I&EC Prod. Res. Dev.* **1969**, *8*, 2.
- [3] Barton, A. F. M. *Chem. Rev.* **1975**, *75*, 731–753.
- [4] Hansen, C. M. *HANSEN SOLUBILITY PARAMETERS*, second ed.; 1998.
- [5] Levine, I. N. *Physical Chemistry*, 5th ed.; 2002.
- [6] James E. Brady, F. S. *Chemistry: Matter and Its Changes*, 4th ed.; 2004.
- [7] Notaro, A.; Frei, A.; Rubbiani, R.; Jakubaszek, M.; Basu, U.; Koch, S.; Mari, C.; Dotou, M.; Blacque, O.; Gouyon, J.; et al. *ChemRxiv. Prepr.* **2019**.
- [8] Notaro, A.; Jakubaszek, M.; Rotthowe, N.; Maschietto, F.; Felder, P. S.; Goud, B.; Tharaud, M.; Ciofini, I.; Bedioui, F.; Winter, R. F.; et al. *ChemRxiv. Prepr.* **2019**.
- [9] Bard, A. J.; Ghosh, P. K. *J. Phys. Chem.* **1984**, *88*, 5519–5526.
- [10] Babu, E.; Muthu, P.; Murali, M.; Sathish, V. *Inorg. Chem. Commun.* **2018**, *98*, 7–10.
- [11] Elemans, J. A. A. W.; Gelder, D.; Rowan, E.; Nolte, R. J. M. **1998**, 6–7.
- [12] Siewert, B.; Langerman, M.; Hontani, Y.; Kennis, J. T. M.; Rixel, V. H. S. Van; Limburg, B.; Siegler, M. A.; Saez, V. T.; Kieltyka, R. E.; Bonnet, S. *ChemComm* **2017**, *53*, 11126–11129.
- [13] Sheet, S. K.; Sen, B.; Patra, S. K.; Rabha, M.; Aguan, K.; Khatua, S. *ACS Appl. Mater. Interfaces* **2018**, *10*, 14356–14366.
- [14] Campagna, S.; Giannetto, A.; Serroni, S.; Denti, G.; Trusso, S.; Mallamace, F.; Universita, M.; Agata, V. S.; Inorgánica, C.; Agraria, C.; et al. *J. Am. Chem. Soc.* **1995**, *117*, 1754–1758.
- [15] Deshpande, M. S.; Kumbhar, A. S.; Puranik, V. G.; Selvaraj, K. *Cryst. Growth*

- Des.* **2006**, *6*, 773–748.
- [16] Chen, Y.; Xu, W.; Kou, J.; Yu, B.; Wei, X.; Chao, H.; Ji, L. *Inorg. Chem. Commun.* **2010**, *13*, 1140–1143.
- [17] Whitesides, G. M.; Grzybowski, B. *Science (80-. )*. **2002**, *295*, 2418–2422.
- [18] Glotzer, S. C.; Solomon, M. J.; Kotov, N. A. *AIChE J.* **2004**, *50*.
- [19] Hall, M. D.; Telma, K. A.; Chang, K.-E.; Lee, T. D.; Madigan, J. P.; Lloyd, J. R.; Goldlust, I. S.; Hoeschele, James D. Gottesman, M. M. *Cancer Res.* **2014**, *74*, 3913–3922.
- [20] Patra, M.; Joshi, T.; Pierroz, V.; Ingram, K.; Kaiser, M. *Chem. Eur. J.* **2013**, *19*, 14768–14772.
- [21] Huang, H.; Humbert, N.; Bizet, V.; Patra, M.; Chao, H. *J. Organomet. Chem.* **2017**, *839*, 15–18.
- [22] Dyson, P. J.; Mcgrady, J. E.; Reinhold, M.; Johnson, B. F. G.; Mcindoe, J. S.; Langridge-smith, P. R. R. *J. Clust. Sci.* **2000**, *11*, 391–401.
- [23] Dale, M. J.; Dyson, P. J.; Johnson, B. F. G.; Martin, C. M.; Langridge-smith, P. R. R. *chem comm* **1995**, 1689–1690.
- [24] Zuccaccia, D.; Sabatini, S.; Bellachioma, G.; Cardaci, G.; Clot, E.; Macchioni, A.; Chimica, D.; Uni, V.; Elce, V. *Inorg. Chem. Comun.* **2003**, *42*, 5465–5467.
- [25] Pan, L.; Ho, Q.; Tsutsui, K.; Takahashi, L. *J. Pharm. Sci.* **2001**, *90*, 521–529.
- [26] Malloy, A. *Mater. Today* **2011**, *14*, 170–173.
- [27] Dragovic, R. A.; Gardiner, C.; Brooks, A. S.; Tannetta, D. S.; Ferguson, D. J. P.; Hole, P.; Carr, B.; Redman, C. W. G.; Harris, A. L.; Dobson, P. J.; et al. *Nanomedicine Nanotechnology, Biol. Med.* **2011**, *7*, 780–788.
- [28] Nanoparticle Tracking Analysis; SIZE. *www.malvern.com* **2019**, *NanoSight*:
- [29] Matsumura, Y.; Maeda, H. *CANCER Res.* **1986**, No. December, 6387–6392.

[30] Danhier, F. *J. Control. Release* **2016**, *244*, 108–121.

# Note of Caution for the Behaviour of Metal-based Drug Candidates upon Aqueous Dilution from Stock Solutions

*Anna Notaro,<sup>a</sup> Gilles Gasser,<sup>a,\*</sup> and Annie Castonguay<sup>b,\*</sup>*

<sup>a</sup> Chimie ParisTech, PSL University, CNRS, Institute of Chemistry for Life and Health Sciences, Laboratory for Inorganic Chemical Biology, F-75005 Paris, France.

<sup>b</sup> INRS - Centre Armand-Frappier Santé Biotechnologie, Université du Québec, 531 boul. des Prairies, Laval, Québec, H7V 1B7, Canada.

\* Corresponding author: E-mail: [gilles.gasser@chimeparistech.psl.eu](mailto:gilles.gasser@chimeparistech.psl.eu); WWW: [www.gassergroup.com](http://www.gassergroup.com);  
Phone: +33 1 44 27 56 02; Email: [annie.castonguay@inrs.ca](mailto:annie.castonguay@inrs.ca); WWW: [www.castonguay-group-inrs.com/](http://www.castonguay-group-inrs.com/)  
Phone: +1 450 687 5010

## Table of Contents

1) Figure S1. Calibration curve of <b>[Ru(DIP)<sub>2</sub>(sq)](PF<sub>6</sub>)</b> .....	3
2) Figure S2. Calibration curve of <b>[Ru(DIP)<sub>2</sub>(3-methoxysq)](PF<sub>6</sub>)</b> .....	4
3) Figure S3. NTA size distribution at t = 0 of <b>[Ru(DIP)<sub>2</sub>(3-methoxysq)](PF<sub>6</sub>)</b> .....	5
4) Figure S4. NTA size distribution after 24 h incubation at 28 °C of <b>[Ru(DIP)<sub>2</sub>(3-methoxysq)](PF<sub>6</sub>)</b> .....	6

1)

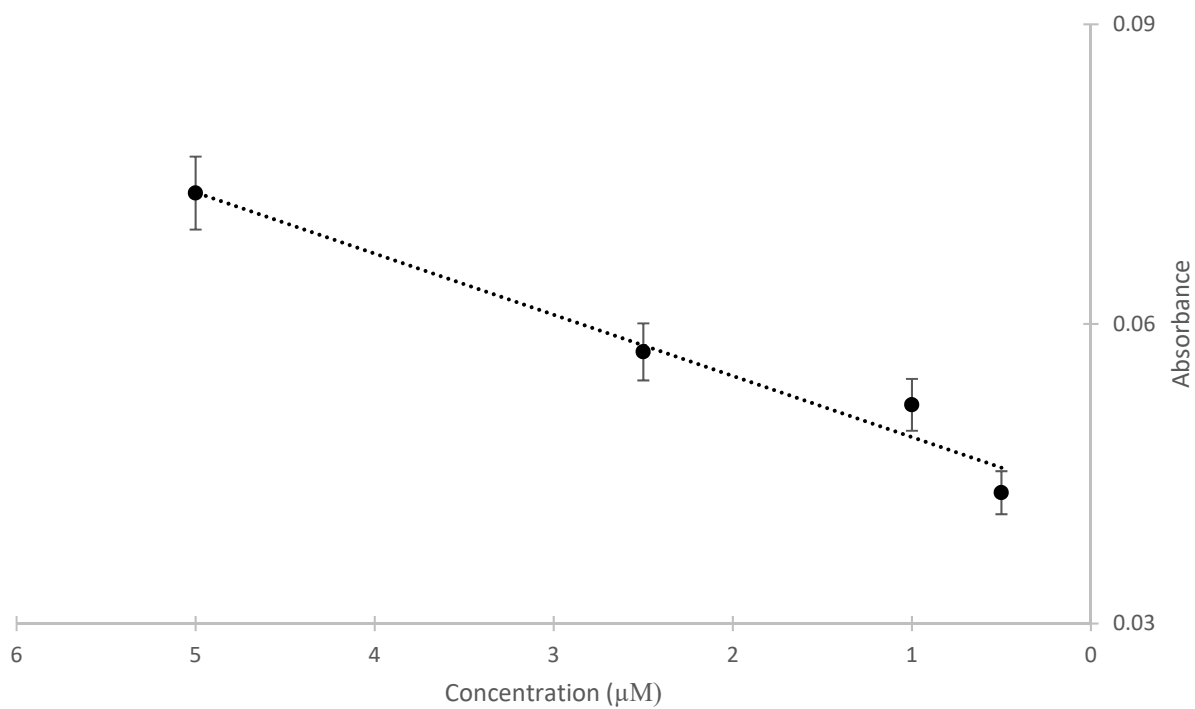


**Figure 1.** Calibration curve obtained by UV-vis absorbance measurements of non-filtered solutions of  $[\text{Ru}(\text{DIP})_2(\text{sq})](\text{PF}_6)$  (5,2.5,1 and 0.5  $\mu\text{M}$ ). Each value is reported with 5% experimental error over the absorbance measurement.

2)

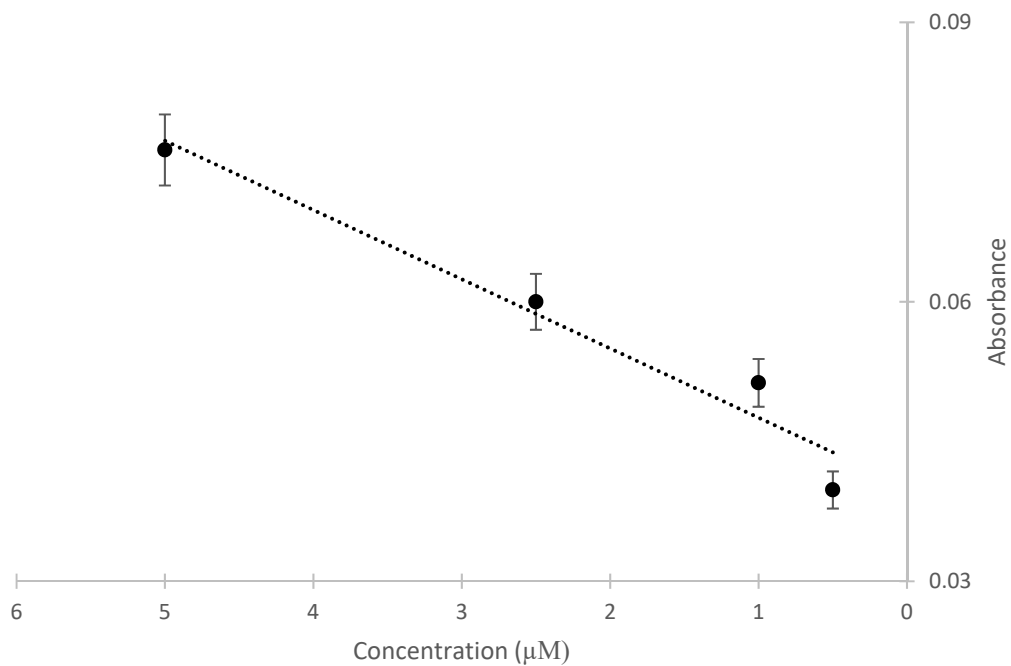


**Figure 2.** Calibration curve obtained by UV-vis absorbance measurements of non-filtered solutions of  $[\text{Ru}(\text{DIP})_2(\text{3-methoxysq})](\text{PF}_6)$  (5,2.5,1 and 0.5  $\mu\text{M}$ ). Each value is reported with 5% experimental error over the absorbance measurement.

3)

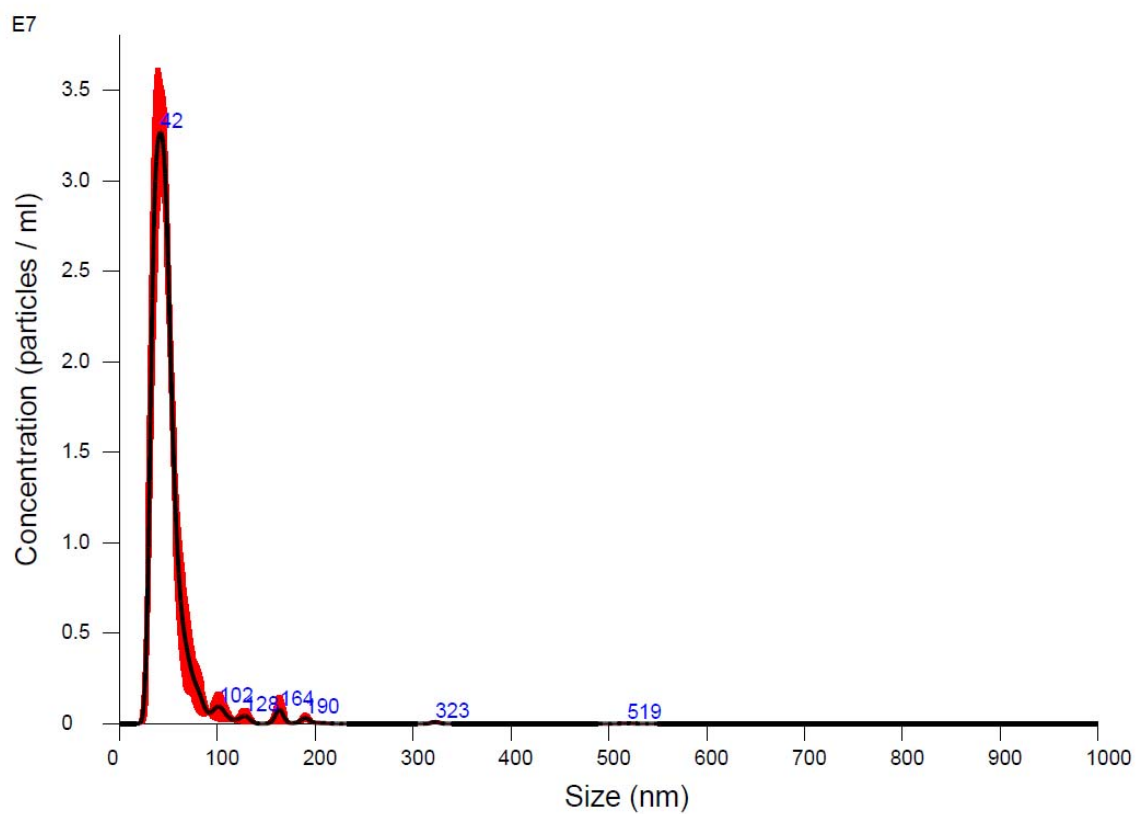


**Figure 3.** NTA size distribution at  $t = 0$  of  $[\text{Ru}(\text{DIP})_2(3\text{-methoxysq})](\text{PF}_6)$   $1\mu\text{M}$  in water-DMSO (1% v/v) mixture.

4)

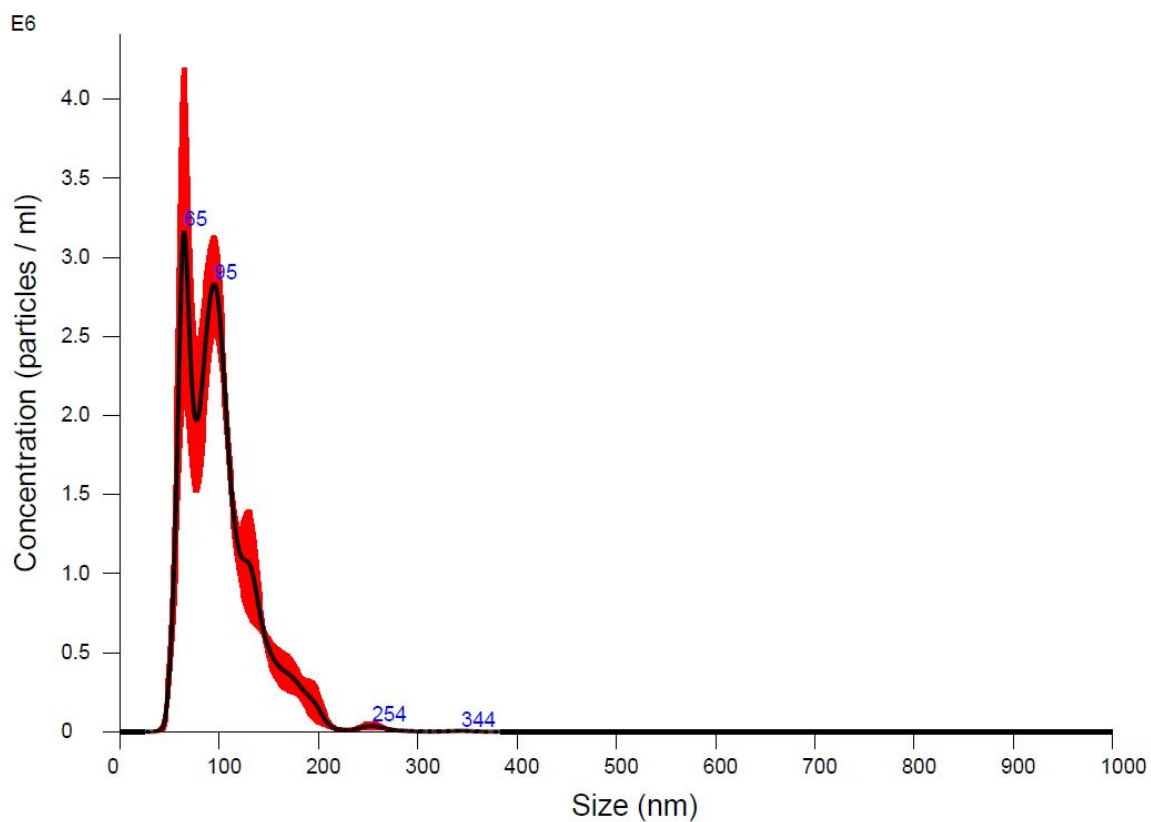


**Figure 4.** NTA size distribution after 24 h incubation at 28 °C of  $[\text{Ru}(\text{DIP})_2(3\text{-methoxysq})](\text{PF}_6)$  1  $\mu\text{M}$  in water-DMSO (1% v/v) mixture.